state formalism, and these we have discussed. The bonding between tellurium and transition-metal atoms is highly covalent. Weak paramagnetism might result from both itinerant and localized electrons.

Acknowledgment. We thank Prof. F. J. DiSalvo and Dr. E. Canadell for helpful comments. Calculations similar to ours were carried out at the Laboratoire de Chimie Theorique, Université de Paris Sud, by E. Canadell and I. El Idrissi. J.-F.H. thanks Dr. R. L. Johnston for sharing his expertise. His stay at Cornell was made possible by a grant from an exchange program between the NSF and the CNRS. W.T. was supported by a Liebig fellowship from the Verband der Chemischen Industrie. The computing equipment at Münster was purchased through a grant by the Deutsche Forschungsgemeinschaft (DFG, Kr 406/9-1). The work at Cornell was supported by NSF Grant DMR85-16616-AO2. The work at Northwestern University was supported by NSF Solid State Chemistry Grants DMR 83-15554 and DMR 88-13623.

Appendix

The parameters used in the calculations are listed in Table I. The tellurium parameters have been chosen to reproduce self-consistent LMTO-ASA calculations in $NiTe_2$.[9] The experimental geometries of $NbNiTe_5$, $NdTe_2$, and $NdTe_3$ were used for all calculations.

A 21K-point set was used in the rectangle irreducible Brillouin zone for the DOS calculations. The plot of the band structure along high-symetry lines has been made using the space group D_{2h}^5-*Pmcm* (*Pmma*, no. 51) to account for the thickness of the two-dimensional $NbNiTe_5$ slab. For $LaTe_2$ and $LaTe_3$ a 27K-point set was used in the irreducible wedge of the Brillouin zone.

Registry No. $NiNbTe_5$, 113671-41-3.

A Designed Fluid Cracking Catalyst with Vanadium Tolerance

C. A. Altomare,*[1] G. S. Koermer,[1] P. F. Schubert,[2] S. L. Suib,[3] and W. S. Willis[3]

Engelhard Corporation, Menlo Park, CN 40, Edison, New Jersey 08818, and Department of Chemistry and Institute of Materials Science, University of Connecticut, Storrs, Connecticut 06268

Received February 6, 1988

A fluid cracking catalyst with two functions, strong acid zeolitic cracking and vanadium passivation, was designed. Vanadium passivation is important for maintaining cracking catalyst performance when processing heavy petroleum feedstocks. The catalyst was made by growing zeolite Y on the external and internal surface of microspheres containing the vanadium trap forsterite. Surface spectroscopy and catalytic results were used to demonstrate that the catalyst was synthesized as designed and that both the cracking function and vanadium trapping function were preserved.

Introduction

Molecular design of materials is a subject of recent interest. The objective of molecular design is to control the physical and chemical properties of a material by carefully controlling the structure and composition of the material. Modification of electrode surfaces to enhance electrocatalytic activity,[4] encapsulation of organometallics in zeolites[5] and layered solids,[6] and control of the size, shape, and composition of optical and electronic materials such as ceramics[7] and second harmonic generators[8] are current areas of interest that involve molecular design of materials.

In this work, molecular design has been applied to cracking catalyst synthesis. Modern cracking catalysts are approximately 70-μm-diameter microspheres containing zeolite Y in a matrix material such as silica alumina. One of the many challenges in catalytic cracking of hydrocarbons is to create materials including both active cracking functions (e.g., zeolite Y) and contaminant scavengers or passivators. Cracking catalyst activity and selectivity are greatly reduced by crude oil contaminants such as nickel, vanadium, and other metals.[9-13] Certain additives incorporated into the catalyst matrix could reduce contaminant effects. Alkaline-earth metal oxides can immobilize vanadium, preventing it from destroying the zeolite, and may also reduce vanadium's undesirable coke and hydrogen making tendencies.[9,10,14-18]

Modern cracking catalyst preparation follows two main routes. The most common involves spray drying cation-

(1) Engelhard Corporation.
(2) Present address: Phillips Petroleum, Bartlesville, OK 74004.
(3) University of Connecticut.
(4) Miller, J. S., Ed. *Chemically Modified Surfaces in Catalysis and Electrocatalysis*; ACS Symposium Series 192; American Chemical Society: Washington, DC, 1982. Zak, J.; Kuwana, T. *J. Electroanal. Chem. Interfacial Electrochem.* **1983**, *150*, 645-664.
(5) Zerger, R. P.; McMahon, K. C.; Seltzer, M. D.; Michel, R. G.; Suib, S. L. *J. Catal.* **1986**, *99*, 498-505.
(6) Pinnavia, T. J. *Science* **1983**, *220*, 365-471.
(7) Lackey, W. J.; Stinton, D. P.; Cerny, G. A.; Scaffhauser, A. C.; Fehrenbacher, L. L. *Adv. Ceram. Mater.* **1987**, *2*, 24-30.
(8) Eddy, M. M.; Gier, T. E.; Keder, N. L.; Stucky, G. D.; Cox, D. E.; Bierlein, J. D.; Jones, G. *Inorg. Chem.* **1988**, *27*, 1856-1858.
(9) Schubert, P. F. *Prepr.—Am. Chem. Soc., Div. Pet. Chem.* **1987**, *32*, 673-676.
(10) Schubert, P. F.; Altomare, C. A. *ACS Symp. Ser.* **1988**, *375*, 182-194.
(11) Occelli, M. L.; Kowalczyk, D. C.; Kibby, C. L. *Appl. Catal.* **1985**, *16*, 227-236.
(12) Grane, H. R.; Conner, J. E.; Masologites, G. P. *Proc., Am. Pet. Inst., Sect. 3* **1961**, *41*, 241-246.
(13) Rothrock, J. J.; Birkhimer, E. R.; Leum, L. N. *Ind. Eng. Chem.* **1957**, *49*, 272-276.
(14) Wormsbecher, R. F.; Peters, A. W.; Maselli, J. M. *J. Catal.* **1986**, *100*, 130-137.
(15) Occelli, M. L. *Prepr.—Am. Chem. Soc., Div. Pet. Chem.* **1987**, *32*, 658-662.
(16) Bell, V. A.; Schubert, P. F.; Turner, G.; Jacobs, V. Federation of Analytical Chemistry and Spectroscopy Societies, Meeting XIV, Detroit, Oct 1987.
(17) Mitchell, B. R.; Vogel, R. F. U.S. Patent 4,451,355, 1984.
(18) Kugler, E. L.; Rhodes, R. P. U.S. Patent 4,743,358, 1988.

0897-4756/89/2801-0459$01.50/0

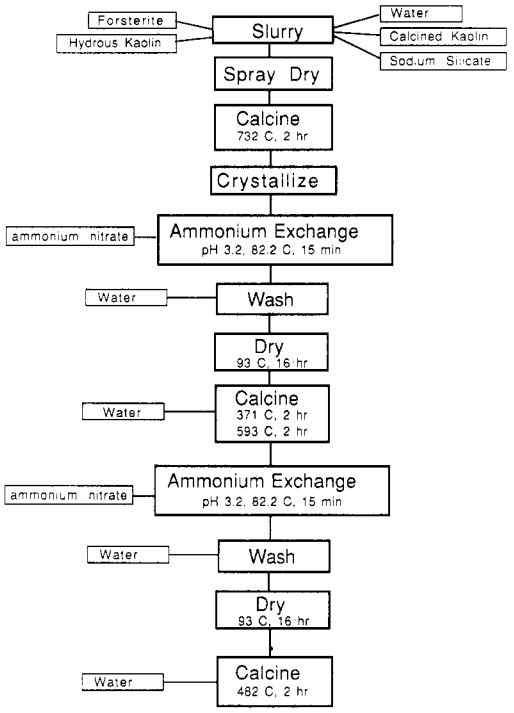

Figure 1. Catalyst synthesis scheme.

exchanged zeolite Y with a silica–alumina sol or gel binder[19,20] into microspheres. The silica–alumina binder is considered the matrix.

The other approach is to spray dry kaolin clay into microspheres.[21,22] These microspheres are calcined at high temperature and then zeolite is crystallized in the resulting porous microspheres. The zeolitic microspheres are cation exchanged and further processed if desired. Catalysts prepared by this second method have advantages in hardness, attrition resistance, matrix stability, and zeolite accessibility.

In the second approach, contaminant scavengers added to the kaolin matrix might hinder zeolite growth or change the cracking performance of the zeolite. Furthermore, zeolite growth on the exposed microsphere surface may obscure the metals trap, hindering its function. We report here that zeolite Y can be grown in the presence of a magnesium-based vanadium scavenger with retention of both cracking activity by the zeolite and vanadium passivation by the magnesium additive.

Experimental Section

A. Catalyst Preparation. Catalysts with and without the vanadium scavenger forsterite were prepared by similar methods outlined in Figure 1.

1. Forsterite-Containing Catalyst (Catalyst I). This catalyst was prepared by spray drying an aqueous slurry (60% solids) to form microspheres with a typical particle size for fluid cracking catalysts (average particle size of about 70 μm). The slurry was composed of the mineral forsterite, obtained from Ward's Geology Earth Sciences, ground to −325 mesh, finely divided hydrous kaolin (ASP 600, a commercially available hydrous kaolin described in Engelhard Technical Bulletin No. TI-1004), Satintone 1, a finely divided fully calcined kaolin (calcined past its characteristic exotherm), sodium silicate, and water. The weight ratio of the mineral components was 20% forsterite, 40% hydrous kaolin, and 40% fully calcined kaolin. The weight of added silica from sodium silicate equaled 5% of the total weight of the combined minerals.

Spray-dried microspheres were calcined at 732 °C for 2 h to convert the hydrous kaolin to metakaolin while leaving the fully calcined kaolin virtually unaffected. The calcined microspheres contained 9.7% MgO in the form of forsterite.

Zeolite Y was synthesized in the calcined microspheres by published procedures.[21,23] The zeolite crystallization gave a material with 45% zeolite Y (unit cell size: 24.68 Å). Catalyst surface area, as measured by the BET method using nitrogen as the adsorbate, was 448 m^2/g. The product also contained 8.7% MgO. The apparent net decrease in bulk MgO content is the result of an overall increase in product weight from zeolite crystallization.

A reduced unit cell size (zeolite Y) version of the catalyst was prepared. First, the catalyst was treated with ammonium nitrate to remove sodium ions. The catalyst was added to a beaker of hot ammonium nitrate solution with constant agitation; 3.5 g of 23% ammonium nitrate was used per gram of catalyst. The resulting slurry was maintained at a pH of 3.2 and a temperature of 82.2 °C for 15 min. The treated catalyst was filtered on a Büchner filter, washed with water, and oven dried at 93 °C overnight

The dried catalyst was calcined twice to reduce the zeolite unit cell size. The first calcination was at 371 °C for 2 h. Water was added to the catalyst before calcination so that the added water plus the moisture content of the catalyst was 25% of the total weight. The second calcination was at 593 °C for 2 h, again with added water. After this calcination, the catalyst BET surface area using nitrogen as an adsorbate was 465 m^2/g, and the zeolite unit cell size was 24.62 Å.

The catalyst was treated again with ammonium nitrate to reduce the soda content to below 0.5%. This procedure was similar to the procedure above except that 2.85 g of 18% ammonium nitrate was used per gram of catalyst. The catalyst was filtered, washed with water, and dried overnight at 93 °C. Finally, the catalyst was calcined at 482 °C for 2 h. Water was added as above. Finished catalyst chemical and physical properties are in Table I.

2. Nonforsterite Catalyst (Catalyst II). A catalyst without forsterite was prepared by the method described above except no forsterite was added. The relative levels of the other solids spray dried were increased proportionally. Chemical and physical properties of finished catalyst II are in Table I.

B. Catalyst Testing. 1. Steam Deactivation. Fluid cracking catalysts are subjected to a high-temperature steam environment in the FCC (fluid catalytic cracker) regenerator. This results in catalyst aging and deactivation.[19] This aging process is simulated in the laboratory by steam deactivation.[21] Steam-deactivated catalyst samples were prepared by fluidizing the catalyst in 100% steam at 1 bar for 4 h at 788 °C.

Steam-deactivated catalysts containing Ni and V were prepared by fluidizing a sample in a 90% steam–10% air mixture at 788 °C and 1 bar for 4 h.

2. Metals Impregnation. Nickel- and vanadium-contaminated catalyst samples were prepared by impregnation with metal naphthenates according to a method previously described.[24]

Table I. Unsteamed Physical and Chemical Properties of Catalysts

	catalyst	
	I	II
Na_2O, wt %	0.43	0.46
MgO, wt %	6.67	0.02
Fe_2O_3, wt %	2.31	0.45
SiO_2, wt %	54.7	57.0
Al_2O_3, wt %	34.0	39.5
surf. area, m^2/g	454	444
unit-cell size, Å	24.60	24.62

(19) Venuto, P. B.; Habib, E. T. Jr. *Fluid Catalytic Cracking with Zeolite Catalysts*; Marcel Dekker: New York, 1979; and references therein.

(20) Stiles, A. B. *Catalyst Manufacture*; Marcel Dekker: New York, 1983; and references therein.

(21) Brown, S. M.; Durante, V. A.; Reagan, W. J.; Speronello, B. K. U.S. Patent 4,493,902 1985.

(22) Haden, W. L.; Dzierzanoski, F. J. U.S. Patent 3,657,154, 1972.

(23) Mitchell, B. R. *Ind. Eng. Chem. Prod. Res. Dev.* **1980**, *19*, 209–213.

3. Catalytic Evaluation. Catalyst performance was assessed by a modified ASTM microactivity test (MAT) described previously.[21] The MAT is the standard method for assessing the activity and selectivity of cracking catalysts in most cracking catalyst laboratories. The ability of the MAT to accurately rank FCC catalysts for activity and selectivity has been reviewed recently.[25]

MAT conditions were 488 °C initial temperature, 15 WHSV (weight hourly space velocity), 6.0 g of catalyst, and a 5.0 catalyst-to-oil ratio. The feedstock was a metals-free midcontinent gas oil (API gravity 29.3). Conversions are reported as weight percent converted to material boiling below 216 °C plus coke. Activity is defined[24] as (wt % conversion)/(100 - wt % conversion).

C. Surface Science Studies. 1. X-ray Photoelectron Spectroscopy (XPS). Experiments were done with a Leybold-Heraeus LHS-10 spectrometer equipped with a dual-anode Mg/Al source. Samples were pressed into indium foil to minimize charging effects. Analysis of the data suggests that charging effects have been minimized on the basis of binding energy positions. Standard curve resolution methods were used to determine binding energies and for deconvolution of broad peaks. Data in Tables I and IV were normalized to silicon. Details concerning these procedures can be found elsewhere.[26]

2. Secondary Ion Mass Spectrometry (SIMS). Experiments were done with a Balzers quadrupole mass spectrometer with mass capabilities to 500 mass units. All experiments were done in the so-called static mode by using low beam currents (<1 μA). All sputtering was done with an Ar^+ ion beam. Pressures during analyses were 1×10^{-7} mbar.

Results and Discussion

Previous studies on the effects of contaminants on cracking catalysts showed that in the presence of steam and air, vanadium migrates from the surface of a nonzeolitic catalyst microsphere into the bulk or inner surface of the microsphere when elements such as magnesium are present.[24] It is believed that magnesium compounds react with vanadium oxide(s) to form stable magnesium vanadates such as $Mg_3(VO_4)_2$.[27] The formation of these species prevents further migration of vanadium to microspheres with zeolite, thus minimizing zeolite destruction by vanadium and preserving catalyst activity. We reasoned that the zeolitic cracking and vanadium trapping functions could be combined into a single microsphere and that a known vanadium trap such as forsterite[28] (magnesium orthosilicate) could be used to trap vanadium even if the outer and inner surfaces of the microsphere were covered by zeolite. However, the effects of forsterite on zeolite growth and stability were unclear. This is an issue because the ions present in a zeolite growth medium can have a large effect on zeolite formation.[29] In addition, ions present during catalyst steam deactivation or aging influence zeolite hydrothermal stability.

To test our hypothesis, microspheres containing forsterite were spray dried. Zeolite Y was grown successfully on the exterior and interior surfaces of these microspheres by using known procedures. The microspheres containing the zeolite were then ammonium exchanged to remove sodium, and the zeolite was stabilized by hydrothermal calcination.[30] The chemical and physical properties of this material (I) are shown in Table I. It has properties similar to those of a cracking catalyst (II) prepared in the same way without forsterite addition and to those of commercial cracking catalysts. A higher level of iron is present in catalyst I. This results from contaminant iron present in the mineral forsterite.

Table II. XPS Surface Analysis of Catalyst I before Steaming

element	rel abundance[a]	element	rel abundance[a]
O	2.72	Al	0.69
C	0.93	Fe	0.01
Si	1.00	Mg	0.01

[a] Relative to silicon.

Table III. Catalytic Test Results after Steam Deactivation

total metals[a]	conversion[b]	activity
	Catalyst I	
0	77.5	3.44
0	78.6	3.66
6030	70.9	2.43
6030	70.5	2.39
6030	70.8	2.42
6030	70.1	2.35
10840	62.5	1.66
10840	63.5	1.74
10840	64.2	1.79
10840	66.9	2.02
	Catalyst II	
0	80.8	4.20
0	81.9	4.53
5390	74.3	2.89
5390	74.3	2.89
10420	64.2	1.79
10420	64.0	1.78
10420	65.5	1.90
10420	65.7	1.91

[a] Total metals: nickel plus vanadium in ppm; Ni/V = 0.5. [b] Weight percent conversion.

The presence of zeolite Y is demonstrated by the high surface area of the material and the XRD pattern, which exactly matches zeolite Y. Thus we have demonstrated that zeolite Y can be successfully grown on the surface of a material that contains magnesium ions.

Surface analysis of catalyst I by X-ray photoelectron spectroscopy (Table II) prior to calcination shows very little magnesium on the surface. This is consistent with zeolite growth covering the surface of the microsphere. As expected, silicon, oxygen, and aluminum are the major elements present. The Si/Al ratio on the surface of I is about 2, which is in good agreement with the ratio expected from Y zeolite. Upon calcination and zeolite stabilization (zeolite framework dealumination) the Si/Al ratio decreases to 1.4–1.6, indicating that there is less silicon on the surface, i.e., more aluminum is present. Surface enrichment of aluminum is consistent with the reported[31] migration of nonframework zeolite aluminum to the zeolite crystal surface during stabilization.

After a preliminary steam deactivation, the hydrocarbon cracking ability of catalysts I and II was assessed by standard microactivity tests (MAT; Table III, zero metals level). Catalyst I gives a somewhat lower conversion than catalyst II. Nevertheless, catalyst I is still a high-conversion cracking catalyst. For comparison, a conventional commercial cracking catalyst subjected to the same steam deactivation and testing conditions would typically have

(24) Altomare, C. A.; Koermer, G. S.; Martins, E.; Schubert, P. F.; Suib, S. L.; Willis, W. S. *Appl. Catal.* **1988**, *45*, 291–306.
(25) Rawlence, D. J.; Gosling, K. *Appl. Catal.* **1988**, *43*, 213–237.
(26) Willis, W. S.; Suib, S. L. *J. Am. Chem. Soc.* **1986**, *108*, 5657–5659.
(27) Occelli, M. L.; Stencel, J. M. *Prepr.—Am. Chem. Soc., Div. Pet. Chem.* **1987**, *32*, 669–672.
(28) Hall, J. B.; Hirschberg, E. H. *Proc. Annu. Meet., Electron Micros. Soc. Am.* **1987**, *45*, 200–201.
(29) Barrer, R. M. *Hydrothermal Chemistry of Zeolites*; Academic Press: New York, 1982.
(30) Scherzer, J. *ACS Sym. Ser.* **1984**, *No. 248*, 157–200.
(31) Fleisch, T. H.; Meyers, B. L.; Ray, G. J.; Hall, J. B.; Marshall, C. L. *J. Catal.* **1986**, *99*, 117–125.

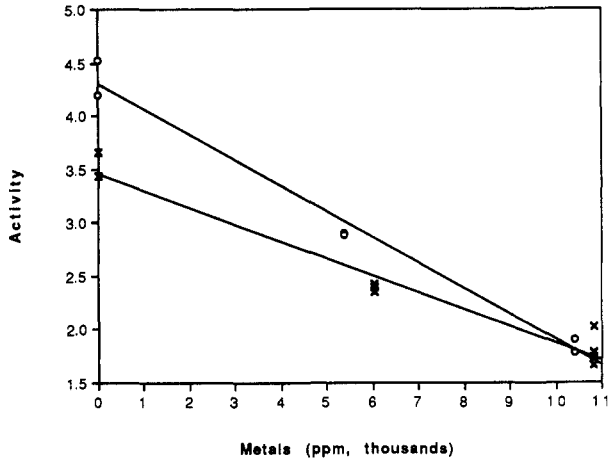

Figure 2. Activity as a function of total metals loading (ppm Ni and V) for catalyst I (×) and catalyst II (○).

Table IV. Forsterite Catalyst Has Reduced Contaminant Coke and Contaminant Hydrogen[a]

catalyst	activity	coke yield	H_2 yield
I	1.66	7.30	0.81
	1.74	7.78	0.86
	1.79	7.56	0.88
	2.02	7.18	0.92
	av 1.80	7.44	0.87
II	1.79	9.33	1.09
	1.78	10.08	1.13
	1.90	9.45	0.99
	1.91	9.76	1.08
	av 1.85	9.66	1.07

[a] Total metals: catalyst I, 10 840 ppm; catalyst II, 10 420 ppm. Ratio of Ni to V approximately 0.5.

70–75% conversion. Thus we conclude that the presence of forsterite reduced cracking activity, but this penalty was within acceptable limits.

To test if forsterite passivates vanadium, we looked at metalated catalyst activity and selectivity as well as the vanadium location on the catalyst. Catalysts I and II were impregnated with vanadium and nickel in a 2:1 weight ratio. Nickel as well as vanadium was included to more closely simulate actual commercial circumstances. Two levels of metals were used. These metal-impregnated catalysts were then steam deactivated, analyzed, and tested. If the vanadium trap is functional, one expects that the activity drop should be less for catalyst I than for catalyst II at the same metals level. In addition, hydrogen and coke yields from catalyst I should be reduced due to less dehydrogenation activity from the vanadium. Finally, our previous results[24] indicate that if the vanadium trapping function is active, vanadium will migrate from the microsphere surface to the particle interior.

Catalytic data in Table III address the activity issue. If the vanadium trap is functional, less zeolite should be destroyed in catalyst I than in catalyst II. Since activity is proportional to zeolite content,[32] this would be reflected in a smaller drop in activity for catalyst I than for catalyst II at the same metals level. Activity as a function of metals level is plotted in Figure 2 for catalysts I and II. A least-squares regression line (shown in Figure 2) for catalyst I has an intercept of 3.46 and a slope of −0.158 per thousand ppm; the line for catalyst II has values of 4.31 and −0.239, respectively. R^2 values are 0.98 (catalyst I) and 0.99

(32) Hayward, C. T.; Koermer, G. S. Presentation at the 10th North American Meeting of the Catalysis Society, May 1987.

Table V. XPS Surface Analysis of Metals[a]-Impregnated Catalyst I before and after Steaming

	steamed	unsteamed
Na/Si	0.04	0.2
Al/Si	0.4	0.7
V/Si	0.15	0.84

[a] Metals levels: 7000 ppm V; 3500 ppm Ni.

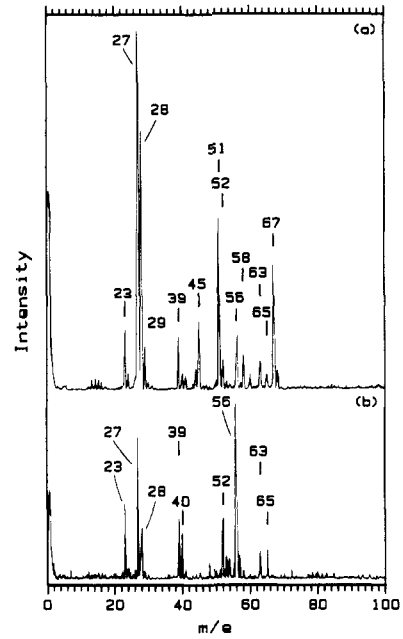

Figure 3. (a) SIMS for catalyst I before steaming. (b) SIMS for catalyst I after steaming.

(catalyst II). The ratio of the slopes is 1.5. Thus we conclude that catalyst I has improved activity maintenance for incremental increases in metals. The most likely explanation for this observation is vanadium trapping by forsterite.

Vanadium poisoning also results in undesirable increases in coke and gas formation.[9] Table IV shows selectivity results for catalysts I and II at essentially the same metals loading and activity. Catalyst I, which contains forsterite, has 20–30% lower coke and gas yields than catalyst II, which has no passivation function. From these data we conclude that the vanadium trapping function is active.

XPS analysis of I after metals impregnation but before steaming showed high levels of surface vanadium (Table V). After steaming, the surface vanadium decreased substantially. This is consistent with previous results[24] and suggests that the vanadium is being trapped by the forsterite. Secondary ion mass spectrometry data for the metal-impregnated sample before steaming shows intense peaks for V+ and VO+ (Figure 3a). However, after steaming, SIMS data show only minute amounts of vanadium species (Figure 3b). These observations are also consistent with trapping of vanadium in the particle interior. Bulk chemical analysis indicated that vanadium was not lost in steaming.

Conclusions

The concept of molecular design was applied to cracking catalyst formulation. A zeolite cracking function was combined with a metals trapping function by growing zeolite on the surface of a matrix that contained forsterite, a known vanadium trap.

Spectroscopic evidence shows that there is no magnesium on the exterior of the catalyst particle and that va-

nadium migration to the particle interior occurs in this system during steaming.

Catalytic evidence shows that the strong acid cracking due to the zeolite is maintained by the catalyst design. In addition, activity and selectivity data in the presence of vanadium indicates that the vanadium trapping function is operative.

Therefore we successfully designed and synthesized a cracking catalyst that combines high zeolitic cracking activity with good vanadium passivation.

Acknowledgment. We thank the Department of Energy, Office of Basic Energy Sciences, Division of Chemical Sciences, and the donors of the Petroleum Research Fund, administered by the American Chemical Society, for partial support of this research through equipment purchase (University of Connecticut).

Registry No. V, 7440-62-2; forsterite, 15118-03-3.

Synthesis, Characterization, and Electropolymerization of Nickel(II) Macrocyclic Compounds Containing Pendant *N*-Alkylpyrrole Substituents

Colin P. Horwitz

Department of Chemistry, Rensselaer Polytechnic Institute, Troy, New York 12180-3590

Received March 8, 1989

Incorporation of pendant *N*-alkylpyrrole moieties onto Ni(II)-containing macrocyclic complexes permits formation of electroactive polymer films that adhere to a Pt electrode surface when the pyrrole moieties are electrochemically oxidized. The polymer films, when placed in solvent and supporting electrolyte with no monomer present, exhibit electrochemical activity resembling the monomer in solution for the Ni(II/III) couple and also voltammetry that corresponds to formation of an *N*-alkylpolypyrrole backbone. The compounds were prepared by reaction of the macrocycle $[Ni[(MeOEthi)_2Me_2[14]tetraeneN_4]]^{2+}$ with 1-(2-aminoethyl)pyrrole, 1-(3-aminopropyl)pyrrole, or 1-(6-aminohexyl)pyrrole. The three different *N*-alkylpyrrole compounds allowed changing the distance between the pyrrole functional group and the macrocycle. The relative rates of electropolymerization and resulting film thicknesses were found to be a function of the alkyl chain length as well as the supporting electrolyte in which the polymer was grown when using acetonitrile as the solvent. Electropolymerization in CH_2Cl_2 showed little dependence on the electrolyte.

The modification of electrode surfaces with transition-metal complex polymer films formed by electropolymerization techniques has received considerable attention in recent years.[1] A variety of potentially practical uses have been suggested for chemically modified electrodes including supported electrocatalysts, solid-state devices, battery electrolytes, and others.[2] Much of the understanding of the fundamental electrochemical properties of polymer-modified electrodes (PMEs) necessary for producing practical devices has been elucidated by utilizing films derived from vinyl-substituted ruthenium and osmium polypyridyl complexes.[3] In conjunction with continuing studies on the electrochemical properties of PMEs, attention is now being been focused on finding new electropolymerizable moieties to replace the vinyl substituents and also new metal complexes. It is likely that some of the future advances in PMEs will come from the preparation of polymer films derived from these new complexes.

Electropolymerizable species that might be generally applicable to transition-metal complex polymer film formation by electropolymerization include pyrrole, aniline, and *N*-alkyl-substituted pyrrole and aniline derivatives. Polypyrrole[4] and polyaniline[5] are well-known electronically conducting polymers formed by oxidative electropolymerization of the corresponding monomers. The *N*-alkyl-substituted aniline species form tail-to-tail coupled dimeric species when oxidized electrochemically,[6] and the presence of two of these substituted aniline groups on a metal complex can lead to polymer film formation.[7] Transition-metal complex polymer films derived from porphyrins,[8] cyclams,[9] Schiff bases,[7] metal polypyridyl complexes,[10] and metallocenes[11] have now been prepared utilizing

(1) (a) Murray, R. W. *Electroanal. Chem.* **1984**, *13*, 191. (b) Murray, R. W.; Ewing, A. G.; Durst, R. A. *Anal. Chem.* **1987**, *59*, 379A. (c) Bard, A. J. *J. Chem. Educ.* **1983**, *60*, 302. (d) Wrighton, M. S. *Science* **1986**, *231*, 32.

(2) Swalen, J. D.; Allara, D. L.; Andrade, J. D.; Chandross, E. A.; Garoff, S.; Israelachvili, J.; McCarthy, T. J.; et al. *Langmuir* **1987**, *3*, 932.

(3) (a) Abruna, H. D.; Denisevich, P.; Umana, M.; Meyer, T. J.; Murray, R. W. *J. Am. Chem. Soc.* **1981**, *103*, 1. (b) Meyer, T. J.; Sullivan, B. P.; Caspar, J. V. *Inorg. Chem.* **1987**, *26*, 4147. (c) Calvert, J. M.; Schmehl, R. H.; Sullivan, B. P.; Facci, J. S.; Meyer, T. J.; Murray, R. W.; *Ibid.* **1983**, *22*, 2151. (d) Guadalupe, A. R.; Usifer, D. A.; Potts, K. T.; Hurrell, H. C.; Mogstad, A.-E.; Abruna, H. D. *J. Am. Chem. Soc.* **1988**, *110*, 3462.

(4) (a) Diaz, A. F.; Castillo, J. I.; Logan, J. A.; Lee, W.-Y. *J. Electroanal. Chem.* **1981**, *129*, 115. (b) Feldman, B. J.; Burgmayer, P.; Murray, R. W. *J. Am. Chem. Soc.* **1985**, *107*, 872. (c) Feldberg, S. *Ibid.* **1984**, *106*, 4671. (d) *Handbook of Conducting Polymers*; Skotheim, T. A., Ed.; Marcel Dekker: New York, 1986.

(5) (a) Wei, Y.; Focke, W. W.; Wnek, G. E.; Ray, A.; MacDiarmid, A. G. *J. Phys. Chem.* **1989**, *93*, 495. (b) Huang, W.-S.; Humphrey, B. D.; MacDiarmid, A. G. *J. Chem. Soc., Faraday Trans. 1* **1986**, *82*, 2385. (c) MacDiarmid, A. G.; Chiang, J. C.; Richter, A. F.; Somasiri, N. L. D. In *Conducting Polymers*; Alcacer, L.; Ed.; Reidel: Dordrecht, Holland, 1987.

(6) (a) Hand, R. L.; Nelson, R. F. *J. Am. Chem. Soc.* **1974**, *96*, 850. (b) Mizoguchi, T.; Adams, R. N. *Ibid.* **1962**, *84*, 2058.

(7) Horwitz, C. P.; Murray, R. W. *Mol. Cryst. Lig. Cryst.* **1988**, *160*, 389.

(8) Bedioui, F.; Merino, A.; Devynck, J.; Mestres, C.-E.; Bied-Charreton, C. *J. Electroanal. Chem.* **1988**, *239*, 433.

(9) Collin, J.-P.; Sauvage, J.-P. *J. Chem. Soc. Chem. Commun.* **1987**, 1075.

0897-4756/89/2801-0463$01.50/0